



# Molybdenum(VI) complexes with tridentate Schiff base ligands derived from isoniazid as catalysts for the oxidation of sulfides: synthesis, X-ray crystal structure determination and spectral characterization

Hadi Kargar<sup>1</sup>

Received: 26 May 2021 / Accepted: 20 July 2021  
© Iranian Chemical Society 2021

## Abstract

Two new complexes, including  $[\text{MoO}_2(\text{L}^1)(\text{CH}_3\text{OH})]$  and  $[\text{MoO}_2(\text{L}^2)(\text{CH}_3\text{OH})]$ , with tridentate ONO-donor Schiff base ligands ( $\text{H}_2\text{L}^1$ : (*E*)-*N'*-(2-hydroxy-3-methoxybenzylidene)isonicotinohydrazide and  $\text{H}_2\text{L}^2$ : (*E*)-*N'*-(5-chloro-2-hydroxybenzylidene)isonicotinohydrazide) have been synthesized and characterized spectroscopically through FT-IR and  $^1\text{H-NMR}$  and by elemental analyses. Their solid-state structures were also confirmed by single-crystal X-ray diffraction (SC-XRD) technique. These tridentate Schiff base ligands coordinated to the metal ion via phenolate oxygen, imine nitrogen and enolic oxygen atoms. In the complexes, the molybdenum center adapts a slightly distorted octahedral geometry, by using three O,N,O-donor atoms of the tridentate ligands, methanol and an oxo group employing the axial positions, while another oxo group makes the equatorial plane. Moreover, the complexes were utilized in oxidizing the different sulfides as an efficient homogeneous catalyst in the presence of *tert*-butyl hydroperoxide (TBHP) as an oxidizing agent in 1,2-dichloroethane (DCE) as a solvent under refluxed conditions. This method has numerous ascendancies such as high yield, short reaction time and excellent selectivity to produce corresponding sulfoxides without overoxidation to sulfones.

**Keywords** Molybdenum · Crystal structure · ONO-tridentate Schiff base · Homogeneous catalyst

## Introduction

Isoniazid (INH) is the N-containing heterocyclic compound, which has the main constituents of natural products and has remarkable medicinal applications [1–3]. INH got much more attention due to the exhibition of various kinds of biological activities like antibacterial, anti-analgesic, antiviral, antitumor, antifungal and anti-convulsant [4–9]. INH is also used as an antitubercular drug since more than 65 years [10]. One of the promising properties of INH is its coordination with the metal cations through pyridinic nitrogen and/or carbonylic oxygen, and nitrogen atoms of the hydrazine part [11]. Another point of interest is that it can be treated with several alkanals to generate Schiff bases, which can

subsequently be reacted with metal salts to give Schiff base metal complexes [12]. Hence, the introduction of azomethine group is responsible for the exhibition of diverse kinds of biological activities due to enhancement of therapeutic effectiveness [13–15].

There are various challenges in the field of chemical sciences, and the top most is the enhancement of catalytic activity, reproducibility and selectivity of the catalytic species. The catalytic activity and selectivity rely on the reagents used and the conditions provided [16]. It is necessary to attain the maximum rate of conversion along with the increased yield and to minimize the waste products generated during chemical synthesis [17]. The parameters that have strong influence for the selective catalytic conversions include the type of oxidant, amount of the catalyst and temperature of reaction [18].

There are many traditional processes, which are commonly used for the oxidation of sulfides to sulfoxides by employing nitric acid, ozone, dinitrogen tetroxide, hydrogen peroxide, peracids, *tert*-butyl hydroperoxide, etc., as a

✉ Hadi Kargar  
h.kargar@ardakan.ac.ir; hadi\_kargar@yahoo.com

<sup>1</sup> Department of Chemical Engineering, Faculty of Engineering, Ardakan University, P.O. Box 184, Ardakan, Iran

source of oxygen [19]. Sulfoxides have a lot of applications in pharmacy as well as in engineering for the production of polymers [20–22]. The direct route for the production of sulfoxides is selective oxidation [23]. A wide variety of supported metal oxides and homogeneous transition metal complexes have been documented in the literature for the oxidation of sulfoxides [24–26]. However, none of these methods give an ideal combination of simplicity as well as selectivity. The selective oxidation of organic moieties by the metal complexes becomes a turning point not only for the synthesis of organic compounds but also for bioinorganic modelling of the oxygen transfer metalloenzymes.

Molybdenum is a very promising transition metal of the second row of transition series, which is involved in life-sustaining processes as it is an important component of enzymes involved in redox reactions [27–29]. The biochemical potential of molybdenum is due to its capability to form complexes with a variety of ligands having O, N and O donor sites [30, 31]. In addition to the biological applications, molybdenum is also equally important from a catalytic perspective. Mononuclear dioxomolybdenum(VI) complexes have played an auspicious role for numerous chemical reactions like hydrodesulfurization, olefin metathesis/epoxidation, sulfoxidation and oxidation of benzylic alcohols [32, 33].

Among the transition metal catalysts, the molybdenum-based complexes proved themselves to be highly active for the selective oxidation reactions by using peroxides as a source of oxygen. Hydrazones obtained by the condensation of isonicotinic acid hydrazides with *o*-hydroxybenzaldehyde derivatives are an important class of Schiff base ligands, which have great tendency to form transition metal complexes [34]. These tridentate ONO-donor-type ligands can stabilize the metal in high oxidation states, which make them stable to bear the drastic catalytic reaction conditions [35].

In the view of excellent catalytic potential of dioxomolybdenum complexes for sulfoxidation and in continuation of our previous works in oxidation reactions [36–39], we have aimed to synthesize and characterize isoniazid-based molybdenum complexes to explore its catalytic efficiency.

## Experimental

### Materials and methods

Aldehydes and isonicotinic hydrazide were acquired from Sigma-Aldrich and Merck, respectively. The dioxomolybdenum salt,  $[\text{MoO}_2(\text{acac})_2]$ , was synthesized by using ammonium molybdate and acetylacetone as described previously [40]. All solvents and other reagents employed in the current work were of HPLC grade and used as obtained without adapting any further purification step. BRUKER AVANCE

500-MHz spectrophotometer was used for recording NMR spectra of the synthesized compounds by using  $\text{DMSO-}d_6$  as a deuterated solvent at ambient temperature. Tetramethylsilane (TMS) was used as an internal standard for the comparison of chemical shift values ( $\delta$ ), which are presented in ppm. The Fourier transform infrared spectra were recorded from 4000 to  $400\text{ cm}^{-1}$  in the form of KBr pellets using an IRPrestige-21 spectrophotometer (Shimadzu). The elemental analysis (CHN) of the synthesized compounds was taken down on a LECO CHNS-932 elemental analyzer.

### General procedure for the synthesis of the Schiff base ligands ( $\text{H}_2\text{L}^n$ ) ( $n = 1, 2$ )

ONO-type tridentate Schiff base ligands,  $\text{H}_2\text{L}^n$ , were synthesized by mixing equimolar amounts of isoniazid and the corresponding salicylaldehyde (3-methoxysalicylaldehyde =  $\text{H}_2\text{L}^1$  and 5-chlorosalicylaldehyde =  $\text{H}_2\text{L}^2$ ) in absolute MeOH. The mixed contents were refluxed for about 3 h to get a clear yellow colored solution, which were then left as such for a period of five days until the products were crystallized out in pure form. The elemental analyses and the spectroscopic data clearly confirm the composition of the targeted compounds. The overall preparation of the subjected ligands is shown in Scheme 1.

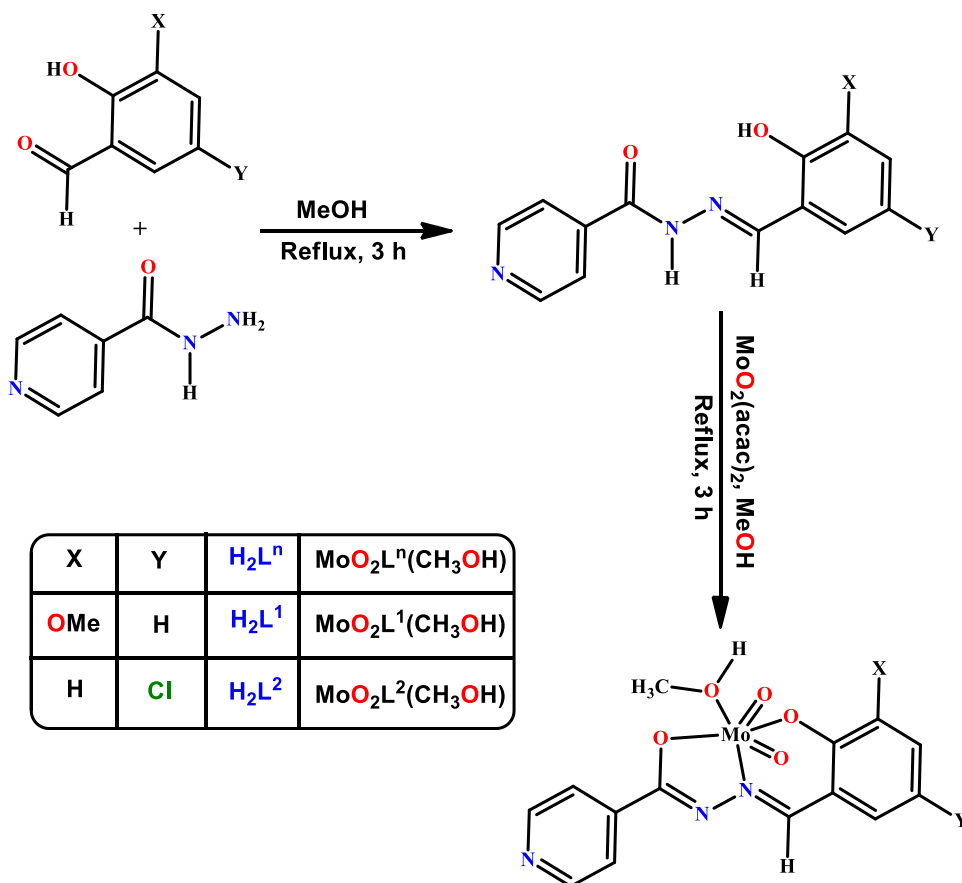
$\text{H}_2\text{L}^1$ ; (*E*)-*N'*-(2-hydroxy-3-methoxybenzylidene)isonicotinohydrazide, Yield: 87%. Calculated for  $\text{C}_{14}\text{H}_{13}\text{N}_3\text{O}_3$ : C 61.99, H 4.83, N 15.49%. Analysis found: C 61.82, H 4.88, N 15.56%. FT-IR (KBr,  $\text{cm}^{-1}$ ): 3200 ( $\nu_{\text{N-H}}$ ); 1689 ( $\nu_{\text{C=O}}$ ); 1602 ( $\nu_{\text{C=N}}$ ); 1566 ( $\nu_{\text{C=C}}$ ); 1246 ( $\nu_{\text{C-O(phenolic)}}$ ); 1064 ( $\nu_{\text{N-N}}$ ).  $^1\text{H NMR}$  (500 MHz,  $\text{DMSO-}d_6$ , ppm): 3.81 [s, 3 H, (-OCH<sub>3</sub>)], 6.82 [1 H, (H-C4), t,  $^3J = 7.9\text{ Hz}$ ], 7.00 [1 H, (H-C3), dd,  $^3J = 7.9\text{ Hz}$ ,  $^4J = 0.9\text{ Hz}$ ], 7.17 [1 H, (H-C5), dd,  $^3J = 7.9\text{ Hz}$ ,  $^4J = 0.9\text{ Hz}$ ], 7.84 [2 H, (H-C10, H-C13), dd,  $^3J = 4.6\text{ Hz}$ ,  $^4J = 1.4\text{ Hz}$ ], 8.69 [1 H, s, (-CH=N)], 8.79 [2 H, (H-C11, H-C12), d,  $^3J = 4.6\text{ Hz}$ ], 11.72 [1 H, s, (-NH)], 12.27 [1 H, s, (-OH)].

$\text{H}_2\text{L}^2$ ; (*E*)-*N'*-(5-chloro-2-hydroxybenzylidene)isonicotinohydrazide, Yield: 91%. Calculated for  $\text{C}_{13}\text{H}_{10}\text{ClN}_3\text{O}_2$ : C 56.64, H 3.66, N 12.86%. Analysis found: C 56.78, H 3.71, N 12.77%. FT-IR (KBr,  $\text{cm}^{-1}$ ): 3171 ( $\nu_{\text{N-H}}$ ); 1680 ( $\nu_{\text{C=O}}$ ); 1620 ( $\nu_{\text{C=N}}$ ); 1548 ( $\nu_{\text{C=C}}$ ); 1284 ( $\nu_{\text{C-O(phenolic)}}$ ); 1066 ( $\nu_{\text{N-N}}$ ).  $^1\text{H NMR}$  (500 MHz,  $\text{DMSO-}d_6$ , ppm): 6.89 [1 H, (H-C2), d,  $^3J = 8.7\text{ Hz}$ ], 7.42 [1 H, (H-C3), dd,  $^3J = 8.7\text{ Hz}$ ,  $^4J = 2.4\text{ Hz}$ ], 7.81 [1 H, (H-C5), d,  $^4J = 2.4\text{ Hz}$ ], 7.83 [2 H, (H-C10, H-C13), d,  $^3J = 5.4\text{ Hz}$ ], 8.64 [1 H, s, (-CH=N)], 8.78 [2 H, (H-C11, H-C12), d,  $^3J = 5.4\text{ Hz}$ ], 11.12 [1 H, s, (-NH)], 12.34 [1 H, s, (-OH)].

### General procedure for the preparation of the complexes

The dioxomolybdenum(VI) complexes of the type  $\text{MoO}_2(\text{L}^n)$  ( $\text{CH}_3\text{OH}$ ) were synthesized by suspending the equimolar

**Scheme 1** The synthetic pathways of  $H_2L^n$  ligands and  $MoO_2(L^n)(CH_3OH)$  complexes



amounts of the respective ligands,  $H_2L^n$  (1 mmol), and  $MoO_2(acac)_2$  (1 mmol, 0.330 g) in 100 mL of methanol in a round-bottom flask with a provision of magnetic bar for steady stirring to attain the uniformity. The resultant suspension was refluxed for approximately 3 h, and then, 2/3rd of the solvent was evaporated to concentrate the mixture, and the remaining contents were cooled down over an ice bath to generate the red-colored crystals appropriate for SC-XRD studies. These crystals were separated by the process of filtration and then washed carefully with  $H_2O$ , MeOH, and  $(C_2H_5)_2O$  separately and finally dried out *in vacuo*.

$[MoO_2(L^1)(CH_3OH)]$  (1) Yield: 83%. Calculated for  $C_{15}H_{15}MoN_3O_6$ : C, 41.97; H, 3.52; N, 9.79%. Analysis found: C, 42.11; H, 3.47; N, 9.64%. FT-IR (KBr,  $cm^{-1}$ ): 3431 ( $\nu_{O-H}$ ) (coordinated methanol); 1600 ( $\nu_{C=N}$ ); 1560 ( $\nu_{C=C}$ ); 1525 ( $\nu_{C=N-N=C}$ ); 1342, 1263 ( $\nu_{C-O}$ ); 1020 ( $\nu_{N-N}$ ); 931 ( $\nu_{O=Mo=O}$ ) *asym*; 906 ( $\nu_{O=Mo=O}$ ) *sym*; 601 ( $\nu_{Mo-O}$ ); 462 ( $\nu_{Mo-N}$ ).  $^1H$  NMR (500 MHz, DMSO- $d_6$ , ppm): 9.00 [s, 1 H, (-CH=N)], 8.75 [d,  $^3J(H,H)=8.9$  Hz, 2 H, (H-C11, H-C12)], 7.86 [d,  $^3J(H,H)=8.9$  Hz, 2 H, (H-C10, H-C13)], 7.33 [d,  $^3J(H,H)=13.2$  Hz, 1 H, (H-C5)], 7.26 [d,  $^3J(H,H)=13.2$  Hz, 1 H, (H-C3)], 7.04 [t,  $^3J(H,H)=13.2$  Hz, 1 H, (H-C4)], 4.10 [q,  $^3J(H,H)=8.7$  Hz, 1 H, -OH (Methanol)], 3.80 [s, 3 H, -OCH<sub>3</sub>, (H-C14)], 3.15 [d,  $^3J(H,H)=8.7$  Hz, 3 H, -CH<sub>3</sub> (Methanol)].

$[MoO_2(L^2)(CH_3OH)]$  (2) Yield: 78%. Calculated for  $C_{13}H_8ClMoN_3O_4$ : C, 38.88; H, 2.01; N, 10.46%. Analysis found: C, 38.96; H, 1.97; N, 10.39%. FT-IR (KBr,  $cm^{-1}$ ): 3431 ( $\nu_{O-H}$ ) (coordinated methanol); 1604 ( $\nu_{C=N}$ ); 1544 ( $\nu_{C=C}$ ); 1525 ( $\nu_{C=N-N=C}$ ); 1344, 1259 ( $\nu_{C-O}$ ); 1014 ( $\nu_{N-N}$ ); 935 ( $\nu_{O=Mo=O}$ ) *asym*; 904 ( $\nu_{O=Mo=O}$ ) *sym*; 601 ( $\nu_{Mo-O}$ ); 462 ( $\nu_{Mo-N}$ ).  $^1H$  NMR (500 MHz, DMSO- $d_6$ , ppm): 8.99 [s, 1 H, (-CH=N)], 8.75 [d,  $^3J(H,H)=9.6$  Hz, 2 H, (H-C11, H-C12)], 7.89 [d,  $^4J(H,H)=4.5$  Hz, 1 H, (H-C5)], 7.86 [d,  $^3J(H,H)=9.6$  Hz, 2 H, (H-C10, H-C13)], 7.58 [dd,  $^3J(H,H)=14.7$  Hz,  $^4J(H,H)=4.5$  Hz, 1 H, (H-C3)], 7.01 [d,  $^3J(H,H)=14.7$  Hz, 1 H, (H-C2)], 4.10 [q,  $^3J(H,H)=8.7$  Hz, 1 H, -OH (Methanol)], 3.15 [d,  $^3J(H,H)=8.7$  Hz, 3 H, -CH<sub>3</sub> (Methanol)].

### Crystallographic data of complexes

The X-ray diffraction data of the complexes 1 and 2 were collected at 296(2) K on STOE IPDS II diffractometer with MoK $\alpha$  radiation. The unit cell parameters refinement, data reduction and correction for *Lp* and decay were performed using X-AREA [41] software. Absorption corrections were applied using MULABS [42] routine in PLATON [43]. The structures were solved by direct methods and refined by the least squares method on  $F^2$  using the SHELXTL program

package [44]. All of the calculations were done by using the PLATON. The non-hydrogen atoms were refined anisotropically, and the carbon-bonded hydrogen atoms were positioned geometrically and refined with a riding model approximation with their parameters constrained to the parent atom with  $U_{iso}(\text{H}) = 1.2$  or  $1.5 U_{eq}(\text{C})$ . The hydrogen atoms bonded with the oxygen atoms in the ligand and complexes were located from the difference Fourier map and constrained to refine with the parent atoms with  $U_{iso}(\text{H}) = 1.5 U_{eq}(\text{O})$ . The crystallographic data and the refinement parameters of **1** and **2** are shown in Table 1.

### General procedure of catalytic sulfoxidation

To a solution of sulfide (1 mmol) in DCE (5 mL), *tert*-BuOOH (TBHP) (2 mmol) and Mo complex (0.01 mmol) were added, and the contents were stirred under refluxed conditions for the specified times. The continuation of the

catalytic conversion was scrutinized by thin-layer chromatography by employing *n*-hexane and ethyl acetate in 5:2 ratio. On the accomplishment of sulfoxidation, the products were separated by column chromatography using over silica gel with *n*-hexane and ethyl acetate (70:30) as an eluent. All of the products were known and also further confirmed by comparison of their physicochemical characteristics with those of authentic samples.

## Results and discussion

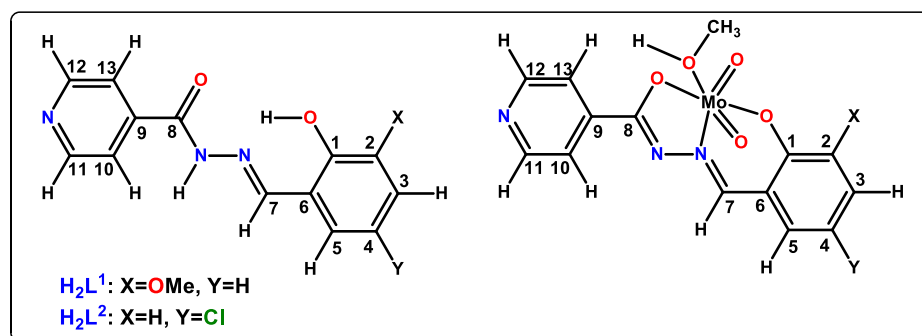
### Synthesis

Hydrazone-based ONO-tridentate Schiff base ligands,  $\text{H}_2\text{L}^n$ , were prepared by treating isoniazid with the corresponding salicylaldehyde in nearly 87–91% yield in methanol. The treatment of  $\text{H}_2\text{L}^n$  with  $\text{MoO}_2(\text{acac})_2$  in equimolar amounts

**Table 1** Crystallographic data and structure refinement parameters for **1** and **2**

Identification code	1	2
Empirical formula	$\text{C}_{15}\text{H}_{15}\text{MoN}_3\text{O}_6$	$\text{C}_{14}\text{H}_{12}\text{ClMoN}_3\text{O}_5$
Formula weight	429.27	433.66
Temperature (K)	293(2)	293(2)
Wavelength (Å)	0.71069	0.71069
Crystal system	Monoclinic	Triclinic
Space group	$P2_1/n$	$P-1$
<i>a</i> (Å)	6.816(5)	6.542(5)
<i>b</i> (Å)	30.411(5)	10.732(5)
<i>c</i> (Å)	7.946(5)	12.913(5)
$\alpha$ (°)	90	68.053(5)
$\beta$ (°)	93.477(5)	83.918(5)
$\gamma$ (°)	90	75.409(5)
Volume (Å <sup>3</sup> )	1644.0(16)	813.7(8)
<i>Z</i>	4	2
Calculated density (Mg/m <sup>3</sup> )	1.734	1.770
Absorption coefficient (mm <sup>-1</sup> )	0.836	1.000
<i>F</i> (000)	864	432
Crystal size (mm)	0.25 × 0.12 × 0.08	0.20 × 0.14 × 0.12
$\theta$ range for data collection (°)	2.65 to 29.17	2.10 to 29.00
Limiting indices	– 8 ≤ <i>h</i> ≤ 9 – 41 ≤ <i>k</i> ≤ 34 – 10 ≤ <i>l</i> ≤ 10	– 8 ≤ <i>h</i> ≤ 8 – 14 ≤ <i>k</i> ≤ 14 – 14 ≤ <i>l</i> ≤ 17
Reflections collected	11,916	8224
Independent reflections	4394 [R(int) = 0.022]	4209 [R(int) = 0.032]
Data/restraints/parameters	4394 / 0 / 228	4209 / 0 / 218
Goodness of fit on $F^2$	1.044	1.043
Final R indices [I > 2σ(I)]	$R_1 = 0.0260$ $wR_2 = 0.0600$	$R_1 = 0.0324$ $wR_2 = 0.0733$
R indices (all data)	$R_1 = 0.0363$ $wR_2 = 0.0627$	$R_1 = 0.0448$ $wR_2 = 0.0768$
Largest diff. peak and hole (e.Å <sup>-3</sup> )	0.398 and -0.494	0.490 and -0.498

**Table 2** Characteristic  $^1\text{H}$  NMR chemical shift values (ppm), peak multiplicity and coupling constant  $J$  (Hz) for the synthesized ligands and their corresponding Mo complexes recorded in  $\text{DMSO-}d_6$



Protons	Ligands	
	$\text{H}_2\text{L}^1$	$\text{H}_2\text{L}^2$
-CH <sub>3</sub>	3.81 (s, 3H)	-
H2	-	6.89 (d, 1H), [ $^3J = 8.7$ Hz]
H4	6.82 (t, 1H), [ $^3J = 7.9$ Hz]	-
H3	7.00 [dd, 1H], [ $^3J = 7.9$ Hz, $^4J = 0.9$ Hz]	7.42 [dd, 1H], [ $^3J = 8.7$ Hz, $^4J = 2.4$ Hz]
H5	7.17 (dd, 1H), [ $^3J = 7.9$ Hz, $^4J = 0.9$ Hz]	7.81 (d, 1H), [ $^4J = 2.4$ Hz]
H10 & H13	7.84 (dd, 2H), [ $^3J = 4.6$ Hz, $^4J = 1.4$ Hz]	7.83 (d, 2H), [ $^3J = 5.4$ Hz]
H7	8.69 (s, 1H)	8.64 (s, 1H)
H11 & H12	8.79 (d, 2H), [ $^3J = 4.6$ Hz]	8.78 (d, 2H), [ $^3J = 5.4$ Hz]
-NH	11.72 (s, 1H)	11.12 (s, 1H)
-OH	12.27 (s, 1H)	12.34 (s, 1H)
Protons	Complexes	
	$\text{MoO}_2\text{L}^1(\text{CH}_3\text{OH})$	$\text{MoO}_2\text{L}^2(\text{CH}_3\text{OH})$
-CH <sub>3</sub>	3.80 (s, 3H)	-
-CH <sub>3</sub> (MeOH)	3.15 (d, 3H), [ $^3J = 8.7$ Hz]	3.15 (d, 3H), [ $^3J = 8.7$ Hz]
-OH (MeOH)	4.10 (q, 1H), [ $^3J = 8.7$ Hz]	4.10 (q, 1H), [ $^3J = 8.7$ Hz]
H2	-	7.01 (d, 1H), [ $^3J = 14.7$ Hz]
H4	7.04 (t, 1H), [ $^3J = 13.2$ Hz]	-
H3	7.26 (d, 1H), [ $^3J = 13.2$ Hz]	7.58 (dd, 1H), [ $^3J = 14.7$ Hz, $^4J = 4.5$ Hz]
H5	7.33 (d, 1H), [ $^3J = 13.2$ Hz]	7.89 (d, 1H), [ $^4J = 4.5$ Hz]
H10 & H13	7.86 (d, 2H), [ $^3J = 8.9$ Hz]	7.86 (d, 2H), [ $^3J = 9.6$ Hz]
H11 & H12	8.75 (d, 2H), [ $^3J = 8.9$ Hz]	8.75 (d, 2H), [ $^3J = 9.6$ Hz]
H7	9.00 (s, 1H)	8.99 (s, 1H)

**Table 3** FTIR spectral data of the ligands and their Mo complexes ( $\text{cm}^{-1}$ )

Assignment	$\text{H}_2\text{L}^1$	$\text{MoO}_2\text{L}^1(\text{CH}_3\text{OH})$	$\text{H}_2\text{L}^2$	$\text{MoO}_2\text{L}^2(\text{CH}_3\text{OH})$
$\nu_{\text{O-H(MeOH)}}$	-	3431	-	3431
$\nu_{\text{N-H}}$	3200	-	3171	-
$\nu_{\text{C=O}}$	1689	-	1680	-
$\nu_{\text{C=N}}$	1602	1600	1620	1604
$\nu_{\text{C=C}}$	1566	1560	1548	1544
$\nu_{\text{C=N=N=C}}$	-	1525	-	1525
$\nu_{\text{C-O(phenolic)}}$	1246	1342	1284	1344
$\nu_{\text{C-O}}$	-	1263	-	1259
$\nu_{\text{N-N}}$	1064	1020	1066	1014
$\nu_{\text{O=Mo=O(asym)}}$	-	931	-	935
$\nu_{\text{O=Mo=O(sym)}}$	-	906	-	904
$\nu_{\text{Mo-O}}$	-	601	-	601
$\nu_{\text{Mo-N}}$	-	462	-	462

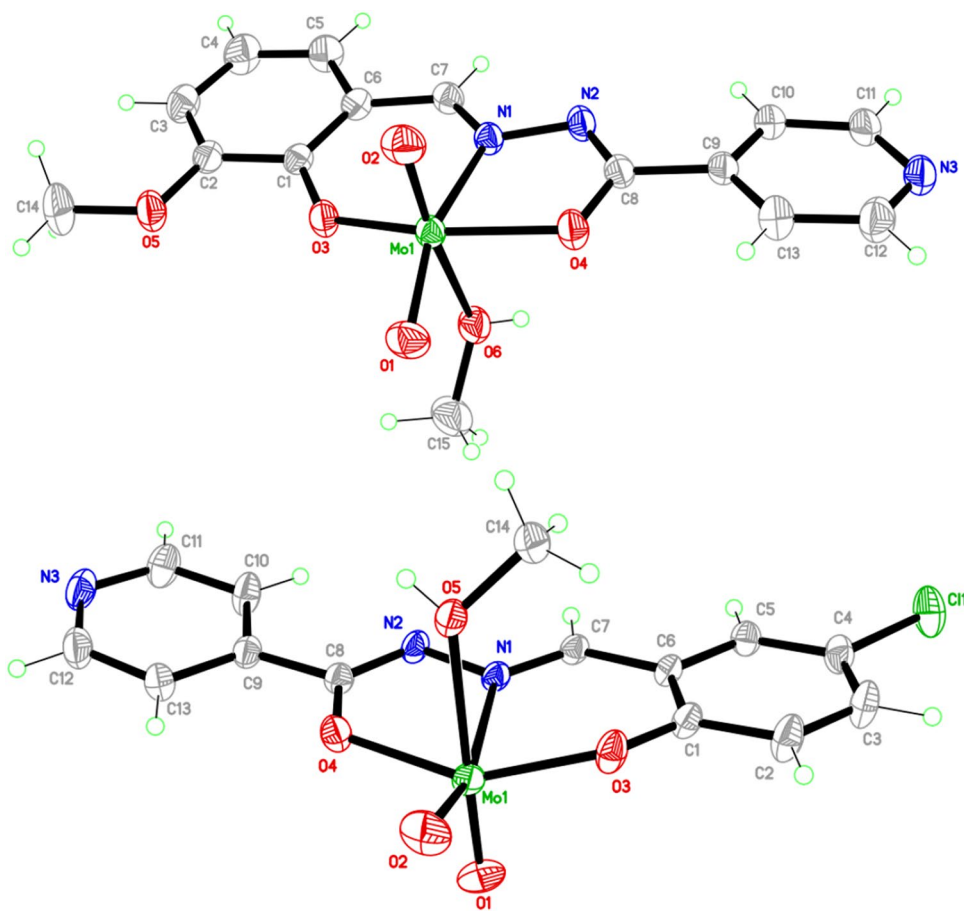
under reflux conditions leads to the synthesis of targeted Mo(VI) complexes. Spectroscopic characterization confirms the proposed molecular formula of the synthesized compounds. Scheme 1 represents the adapted procedure for production of novel Mo(VI) complexes.

## NMR spectra

The  $^1\text{H}$  NMR spectral data of the ligands  $\text{H}_2\text{L}^n$  and their corresponding dioxomolybdenum(VI) complexes in  $\text{DMSO-}d_6$  are furnished in the experimental part, and the spectra are presented in Figures S1–S4. The two important peaks in the spectrum of ligand  $\text{H}_2\text{L}^1$  at  $\delta$  12.27 and  $\delta$  11.72 ppm are assigned to the –OH and –NH protons, respectively. These peaks disappeared on complexation, which is an indication of points of attachment of ligand with metal ion, as well as the occurrence of keto-enol tautomerization on complex formation. In addition to this, there is also a downfield shifting of signal for the azomethine proton (HC=N) of the ligand from  $\delta$  8.69 ppm to  $\delta$  9.00 ppm in the spectrum of the complex on coordination with metal atom. This is because of deshielding of azomethine proton due to the reduction of electronic density at azomethinic bond due to coordination.

This azomethine linkage is also in accordance with the results obtained from the FTIR spectral investigations of  $\text{MoO}_2(\text{L}^1)(\text{CH}_3\text{OH})$ , where the HC=N signal shifts at lower wavenumber as compared to the related free ligand. Hence, in addition to –OH and –NH the nitrogen of HC=N behaves as third site of coordination with metal ion. Hence, the ligand is monobasic and tridentate in nature. The signals for

**Fig. 1** The molecular structures of complexes 1 (up) and 2 (down) with displacement ellipsoids at 50% probability and atom numbering scheme



aromatic protons of the ligands as well as complex come into sight within the expected range. There is no considerable change in the chemical shift values of the aliphatic protons upon complexation. The same kind of pattern is observed for other two ligands and their respective dioxomolybdenum complexes.

The solvent molecule (MeOH) coordinated with the metal atom also shows its presence by giving a quartet for -OH proton at  $\delta$  4.10 ppm [ $^3J(\text{H,H}) = 8.7$  Hz] and a doublet for -CH<sub>3</sub> protons at  $\delta$  3.15 ppm [ $^3J(\text{H,H}) = 8.7$  Hz]. The details of chemical shift values of the ligands and their respective dioxomolybdenum(VI) complexes are presented in Table 2.

### FTIR spectral studies

The FTIR spectra of the ligands and their respective Mo complexes are displayed in Figures S5–S8, and the spectral details are presented in the experimental portion. The indication of binding sites of the ligand from magnetic spectra is further investigated by a conscientious assessment of FTIR spectra of the H<sub>2</sub>L<sup>1</sup> ligand and its corresponding MoO<sub>2</sub>(L<sup>1</sup>)(CH<sub>3</sub>OH) complex. The two flagship regions of interest, i.e., 3200 and 1689 cm<sup>-1</sup>, are there in the spectrum of the ligand. These regions are attributed to the (NH) and (C=O) groups,

which vanish in the complex spectrum. This disappearance is reconcilable by the enolization of the amide functional group due to the replacement of proton with the metal ion [45]. This kind of coordination pattern is further supported by the SC-XRD analysis of the complex. The attachment of MeOH molecule *trans* to the oxo group to occupy the sixth coordination site to stabilize the octahedral geometry is also very common in these types of ligands, especially when the preparation and recrystallization of the complexes are performed in the presence of respective solvents [45, 46].

The emergence of new bands in the region of 1263 cm<sup>-1</sup> is attributed to the enolic (C-O) part. The determining of specific peaks for carbon–carbon double bond of aromatic rings and azomethine in the spectrum of the ligand could not be possible because of the complexity of the spectrum around 1600 cm<sup>-1</sup>. The confirmation of oxo groups in the complex was carried out by appearance of the bands at 931 and 906 cm<sup>-1</sup>, which are ascribed for the asymmetric and symmetric stretching of the *cis*-Mo(O)<sub>2</sub> moiety [47]. Similarly, the presented bands at 601 and 462 cm<sup>-1</sup> are attributed to Mo–O and Mo–N vibrations, respectively, which are in accordance with the previously reported compounds [48]. The coordinated methanol molecule also shows its presence by giving its respective peak at 3431 cm<sup>-1</sup>. The FTIR

**Table 4** The selected bond lengths (Å) and bond angles (°) in **1** and **2** complexes

	1	2
<i>Bond lengths</i>		
Mo(1)–O(1)	1.7096(17)	1.687(2)
Mo(1)–O(2)	1.6907(17)	1.705(2)
Mo(1)–O(3)	1.9354(15)	1.9338(19)
Mo(1)–O(4)	2.0219(14)	2.0161(18)
Mo(1)–O(5)	–	2.316(2)
Mo(1)–O(6)	2.3659(18)	–
Mo(1)–N(1)	2.222(2)	2.242(2)
N(1)–C(7)	1.289(3)	1.279(3)
N(1)–N(2)	1.393(2)	1.396(3)
C(1)–O(3)	1.341(2)	1.295(3)
C(8)–O(4)	1.320(3)	1.324(3)
<i>Bond angles</i>		
O(1)–Mo(1)–O(2)	105.07(9)	105.02(11)
O(1)–Mo(1)–O(3)	102.02(8)	99.01(11)
O(1)–Mo(1)–O(4)	97.62(8)	96.68(10)
O(2)–Mo(1)–O(3)	98.66(8)	102.90(10)
O(2)–Mo(1)–O(4)	96.68(8)	98.14(10)
O(3)–Mo(1)–O(4)	150.90(6)	149.39(8)
O(1)–Mo(1)–N(1)	157.25(7)	90.94(9)
O(2)–Mo(1)–N(1)	96.38(7)	162.41(10)
O(3)–Mo(1)–N(1)	81.77(6)	81.39(7)
O(4)–Mo(1)–N(1)	72.04(6)	72.21(7)

vibrational data for all of the ligands and their corresponding dioxomolybdenum complexes are given in Table 3.

### Illustration of single-crystal analysis of complexes

The simple molecular structures of the Mo complexes are presented in Fig. 1. The complex **1** crystallized out in monoclinic, while complex **2** was appeared in triclinic systems. The space groups found in single-crystal X-ray diffraction analysis are  $P2_1/n$  and  $P-1$  for **1** and **2**, respectively. A tridentate (ONO) Schiff base ligand, two oxo groups at *cis* positions and a coordinated methanol molecule are responsible for the establishment of a distorted octahedral geometry around the molybdenum center. This coordination sphere is further validated by the bond angles associated with the central molybdenum atom, which are given in Table 4. The bond lengths for Mo–N and Mo–O in the complexes are almost analogous to the similar hydrazone-based ligands already reported in the literature [49–51].

The iminic N1–C7 [1.277(6) Å] and N1–N2 [1.408(5) Å] bond lengths were increased after coordination with Mo atom [50]. As commonly revealed from structurally similar complexes, the elongation Mo1–O6 [2.316(3) Å] bond length *trans* to oxo O1 group is an indication of weak coordination of methanol at the axial position, which is due to the strong  $\pi$ -donor character of the oxo group opposite to coordinated methanol [50]. The two Mo=O bond distances and the subtended O(1)=Mo(1)=O(2) are also in accordance with literature values [49–51]. The methoxy-substituted phenyl ring and pyridine ring are

**Fig. 2** Packing diagram of **1** showing formation of zigzag chain of molecules through H-bonding. Only selected H-atoms are shown for clarity

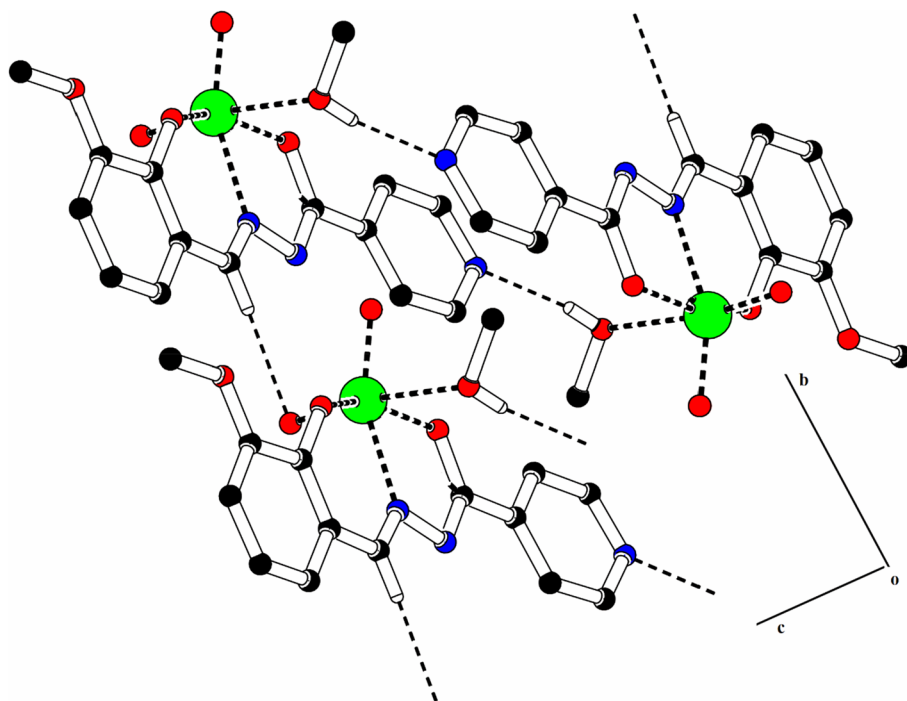


**Table 5** Hydrogen-bond geometry (Å, °) for **1** and **2**

	D—H...A	D—H	H...A	D...A	D—H...A °
1	O6—H6...N3 <sup>i</sup>	0.75	1.98	2.724 (3)	171
	C7—H7A...O2 <sup>ii</sup>	0.93	2.38	3.291 (4)	166
	C11—H11A...O2 <sup>iii</sup>	0.93	2.64	3.148 (4)	115
	C12—H12A...O1 <sup>iv</sup>	0.93	2.61	3.455 (4)	151
	C14—H14B...O1 <sup>v</sup>	0.96	2.66	3.467 (4)	143
	O6—H6...N3 <sup>i</sup>	0.75	1.98	2.724 (3)	171
2	O5—H5...N3 <sup>vi</sup>	0.79	1.92	2.691 (4)	165
	C5—H5A...O1 <sup>vii</sup>	0.93	2.56	3.257 (4)	132
	C7—H7A...O1 <sup>viii</sup>	0.93	2.33	3.181 (4)	151
	C7—H7A...O1 <sup>vii</sup>	0.93	2.60	3.273 (4)	130
	C12—H12A...O2 <sup>ix</sup>	0.93	2.50	3.417 (5)	167

Symmetry codes: (i)  $-x+1, -y, -z+1$ ; (ii)  $x+1, y, z$ ; (iii)  $-x+1, -y, -z+2$ ; (iv)  $-x, -y, -z+1$ ; (v)  $x+1/2, -y+1/2, z+1/2$ ; (vi)  $-x, -y+1, -z$ ; (vii)  $-x, -y+1, -z+1$ ; (viii)  $x-1, y, z$ ; (ix)  $-x+1, -y+1, -z$ ; (x)  $x, -y+3/2, z-1/2$ ; (xi)  $-x, y-1/2, -z-1/2$ ; (xii)  $-x+1, -y+1, -z+1$ ; (xiii)  $-x+1, y-1/2, -z+1/2$

roughly planar with respective root-mean-square deviation of 0.0192 Å and 0.0116 Å in complex **1**. In complex **2**, chloro-substituted phenyl ring and pyridine ring are planar with respective r.m.s deviation of 0.0179 Å and 0.0113 Å. The dihedral angle between methoxy-substituted phenyl ring and pyridine ring is 8.98 (1)° in complex **1**. While the dihedral angle between chloro-substituted phenyl ring and pyridine ring is 11.96 (1)° in complex **2**. The molecules of complex **1** are connected with each other in the form of

dimers via O—H...N bonding to form R<sub>2</sub><sup>2</sup>(18) loop; N-atom of pyridine ring acts as acceptor as shown in Fig. 2 and presented in Table 5. The dimers are interlinked by comparatively weak C—H...O bonding, where one of the oxo groups acts as H-bond acceptor. By the combination of O—H...N and C—H...O bonding, C16 zigzag chain of molecules is formed along [010] direction. Crystal packing of complex **2** is also mainly stabilized by O—H...N bonding to form R<sub>2</sub><sup>2</sup>(18) dimeric loop as shown in Fig. 3 and further stabilized through the comparatively weak C—H...O bonding, likewise offset  $\pi$ ... $\pi$  stacking interaction is found between rings for the further strengthening of the crystal packing but difference between crystal packing of complex **1** and **2** is that in **1** inter-centroid distance for offset  $\pi$ ... $\pi$  stacking interaction between pyridine ring and chelating ring is less than inter-centroid distance between similar rings in complex **2**.

### Catalytic oxidation results

Dioxomolybdenum complexes have widely been utilized as catalysts in various organic transformations, especially in oxidation reactions [52]. The catalytic activity of the prepared Mo complexes was studied in the selective sulfoxidation of several aryl and alkyl sulfides. To optimize the reaction conditions, the oxidation of diphenyl sulfide in the presence of MoO<sub>2</sub>(L<sup>1</sup>)(CH<sub>3</sub>OH) complex was chosen as a model, and the effect of different factors affected on the reaction was investigated.

**Fig. 3** Packing diagram of complex **2**. Only selected H-atoms are shown for clear representation

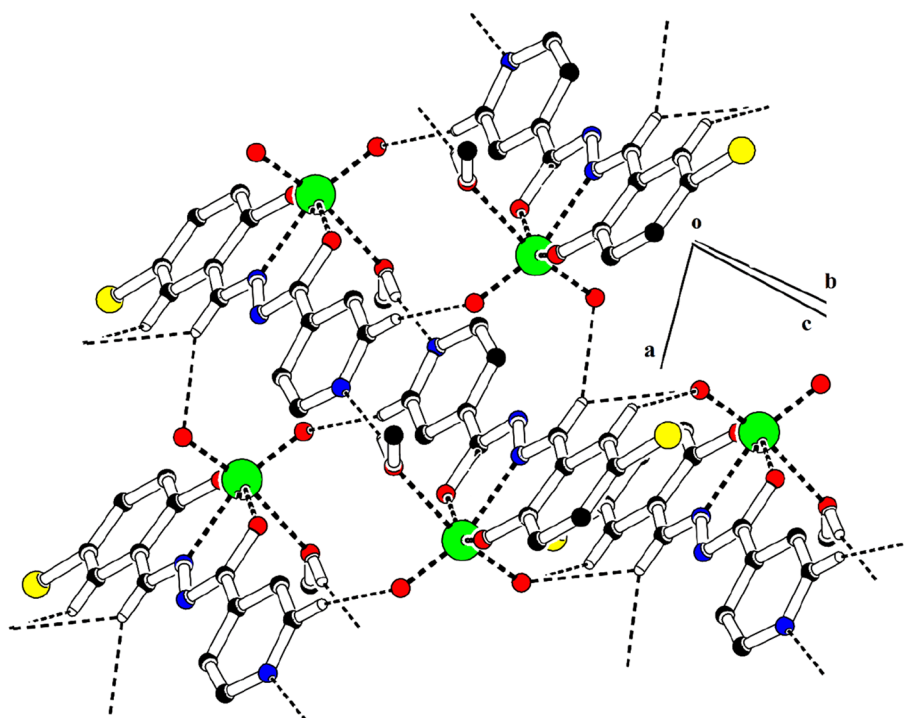


**Table 6** The effect of solvent on the oxidation of diphenyl sulfide with TBHP catalyzed by  $\text{MoO}_2(\text{L}^1)(\text{CH}_3\text{OH})$ .<sup>a</sup>

Entry	Solvent	Conditions	Conversion (%) <sup>b</sup>
1	Toluene	Reflux	70
2	<i>n</i> -Hexane	Reflux	75
3	Acetonitrile	Reflux	85
4	Acetone	Reflux	45
5	Ethanol	Reflux	80
<b>6</b>	<b>DCE</b>	<b>Reflux</b>	<b>100</b>
7	DCE	r.t	Trace
8	DCE	50 °C	35
9	DCE	70 °C	75

<sup>a</sup>Reaction conditions: diphenyl sulfide (1 mmol), TBHP (2 mmol), catalyst (1 mol%), solvent (5 mL), reflux, 1 h

<sup>b</sup>Isolated yields

**Table 7** The effect of type and amount of oxidant on the oxidation of diphenyl sulfide catalyzed by  $\text{MoO}_2(\text{L}^1)(\text{CH}_3\text{OH})$ <sup>a</sup>

Entry	Oxidant	Oxidant amount (mmol)	Conversion (%) <sup>b</sup>
1	No oxidant	0	0
2	$\text{NaIO}_4$	2	85
3	$\text{H}_2\text{O}_2$	2	75
4	UHP	2	65
5	$\text{Bu}_4\text{NIO}_4$	2	10
<b>6</b>	<b>TBHP</b>	<b>2</b>	<b>100</b>
7	TBHP	1	35
8	TBHP	1.5	70
9	TBHP	3	100

<sup>a</sup>Reaction conditions: diphenyl sulfide (1 mmol), oxidant, catalyst (1 mol%), DCE (5 mL), reflux, 1 h

<sup>b</sup>Isolated yields

**Table 8** The effect of amount of catalyst on the oxidation of diphenyl sulfide catalyzed by  $\text{MoO}_2(\text{L}^1)(\text{CH}_3\text{OH})$ <sup>a</sup>

Entry	Catalyst amount (mol%)	Conversion (%) <sup>b</sup>
1	No catalyst	0
2	0.2	50
3	0.5	70
4	0.8	90
5	1	100

<sup>a</sup>Reaction conditions: diphenyl sulfide (1 mmol), TBHP (2 mmol), catalyst, DCE (5 mL), reflux, 1 h

<sup>b</sup>Isolated yields

The reaction was examined in various polar and nonpolar organic solvents in the presence of TBHP as the oxidant and  $\text{MoO}_2(\text{L}^1)(\text{CH}_3\text{OH})$  complex as the catalyst (Table 6). Based on the results, it was found that 1,2-dichloroethane (DCE) is the best solvent for the reaction due to its higher reactivity and selectivity. By changing the reaction temperature in DCE, it can be found that the rate of reaction increases with the increase of temperature and the best result was observed under reflux conditions.

A summary of the effect of different oxidants like  $\text{NaIO}_4$ ,  $\text{H}_2\text{O}_2$ , urea  $\text{H}_2\text{O}_2$  (UHP),  $(\text{Bu})_4\text{NIO}_4$  and TBHP on the oxidation of diphenyl sulfide in the presence of  $\text{MoO}_2(\text{L}^1)(\text{CH}_3\text{OH})$  is presented in Table 7. The reaction did not perform in the absence of oxidant and the best results obtained using TBHP as the source of oxygen. The investigation of the reaction in the presence of different amounts of oxidant showed that the conversion did not complete in the presence of amounts less than 2 mmol of oxidant. The best amount of oxidant for the oxidation to diphenyl sulfoxide was 2 mmol, which completed the reaction and produced sulfoxide as the only product. Higher amount of oxidant did not have much effect on improving the results.

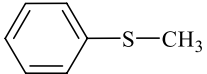
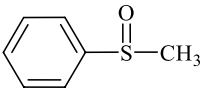
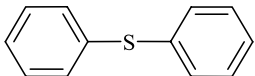
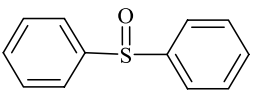
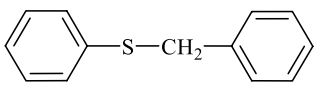
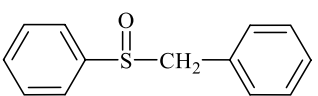
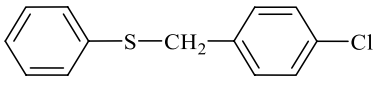
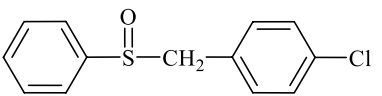
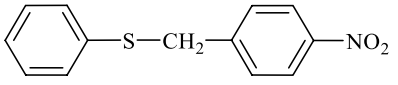
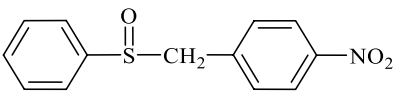
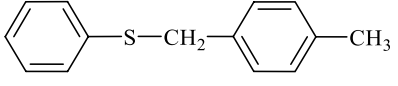
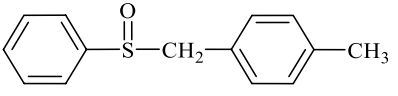
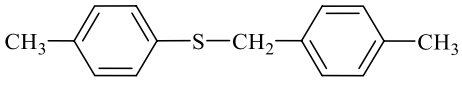
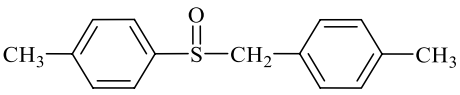
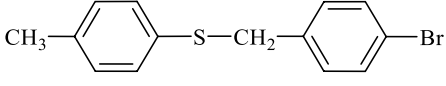
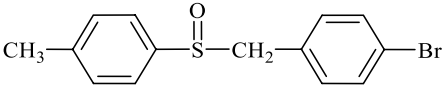
To obtain the optimum amount of the catalyst, the model reaction was performed in the presence of different amounts of  $\text{MoO}_2(\text{L}^1)(\text{CH}_3\text{OH})$ . It was observed that the reaction did not complete in the absence of the catalyst even in higher times. The conversion rate increased with increasing the catalyst amount, and when 1 mol % of the catalyst was applied, the transformation was completed (Table 8).

After optimization of the reaction conditions, oxidation of different sulfides in the presence of  $\text{MoO}_2(\text{L}^n)(\text{CH}_3\text{OH})$  complexes was evaluated under these optimized reaction conditions (Table 9). It is obvious from the table that all studied sulfides were oxidized under this catalytic system and afforded the corresponding sulfoxides in 100% selectivity. It is noteworthy that there is no evidence of overoxidation to produce sulfone in any substrate.

## Conclusion

In the present work, we have described the synthesis of  $[\text{MoO}_2(\text{L}^n)(\text{CH}_3\text{OH})]$  complexes with hydrazone-based Schiff bases derived by the condensation of substituted salicylaldehydes and isoniazid. The synthesized products were characterized spectroscopically and analytically by FTIR,  $^1\text{H}$  NMR and elemental analysis (CHN), and the solid-state structures of the complexes were confirmed by single-crystal X-ray diffraction studies. The tridentate (ONO) Schiff base ligands coordinate to Mo through the phenolic and enolic O atoms and the iminic N atom to display a distorted octahedral geometry around molybdenum center. Moreover, the catalytic efficiencies of the synthesized

**Table 9** Selective oxidation of sulfides with TBHP catalyzed by  $\text{MoO}_2(\text{L}^n)(\text{CH}_3\text{OH})$  complexes.<sup>a</sup>

Entry	Sulfide	Sulfoxide <sup>b</sup>	Time (min.)/ Yield (%) <sup>c</sup>	
			1	2
1			20/92	20/93
2			60/91	60/93
3			30/91	30/93
4			30/92	30/90
5			30/86	30/87
6			20/92	20/93
7			20/88	20/89
8			20/91	20/90

<sup>a</sup>Reaction conditions: sulfide (1 mmol), TBHP (2 mmol), catalyst (1 mol%), DCE (5 mL), reflux conditions

<sup>b</sup>All products were identified by comparison of their physical and spectral data with those of authentic samples

<sup>c</sup>Isolated yield

dioxomolybdenum(VI) were evaluated for the selective sulfoxidation of sulfides using TBHP in 1,2-dichloroethane under reflux conditions. There are numerous advantages of the selected catalytic process like high yield, reduced time for the catalytic conversion and excellent selectivity to produce corresponding sulfoxides without overoxidation to sulfones.

**Supplementary Information** The online version contains supplementary material available at <https://doi.org/10.1007/s13738-021-02355-0>.

**Acknowledgements** The author gratefully acknowledges practical support of this study by Ardakan University.

## Declarations

**Conflict of interest** The authors declare that they have no conflict of interest.

## References

1. S. Vidyacharan, C. Adhikari, V.S. Krishna, R.S. Reshma, D. Sriram, D.S. Sharada, *Bioorg. Med. Chem. Lett.* **27**, 1593 (2017)
2. Z.Q. Li, X.G. Bai, Q. Deng, G.N. Zhang, L. Zhou, Y.S. Liu, J.X. Wang, Y.C. Wang, *Bioorg. Med. Chem.* **25**, 213 (2017)
3. E. Pahlavani, H. Kargar, N. Sepehri Rad, *Zahedan J. Res. Med. Sci.* **17**, 1 (2015)

4. F. Martins, S. Santos, C. Ventura, R. Elvas-Leitao, L. Santos, S. Vitorino, M. Reis, V. Miranda, H.F. Correia, J. Aires-de-Sousa, V. Kovalishyn, D.A.R.S. Latino, J. Ramos, M. Viveiros, Eur. J. Med. Chem. **81**, 119 (2014)
5. L. Xia, Y.F. Xia, L.R. Huang, X. Xiao, H.Y. Lou, T.J. Liu, W.D. Pan, H. Luo, Eur. J. Med. Chem. **97**, 83 (2015)
6. V. Judge, B. Narasimhan, M. Ahuja, D. Sriram, P. Yogeeswari, E.D. Clercq, C. Pannecouque, J. Balzarini, Med. Chem. Res. **21**, 1451 (2012)
7. M. Malhotra, S. Sharma, A. Deep, Med. Chem. Res. **21**, 1237 (2012)
8. G. Nigade, P. Chavan, M. Deodhar, Med. Chem. Res. **21**, 27 (2012)
9. M. Malhotra, V. Monga, S. Sharma, J. Jain, A. Samad, J. Stables, A. Deep, Med. Chem. Res. **21**, 2145 (2012)
10. Y.Q. Hu, S. Zhang, F. Zhao, C. Gao, L.S. Feng, Z.S. Lv, Z. Xu, X. Wu, Eur. J. Med. Chem. **133**, 255 (2017)
11. M. Poggi, R. Barroso, A.J. Costa-Filho, H.B. de Barros, F. Pavan, C.Q. Leite, D. Gambino, M.H. Torre, J. Mex. Chem. Soc. **57**, 198 (2013)
12. A. Kajal, S. Bala, S. Kamboj, N. Sharma, V. Saini, J. Catalysts **2013**, 1 (2013)
13. M.J. Hearn, M.H. Cynamon, M.F. Chen, R. Coppins, J. Davis, H.J.O. Kang, A. Noble, B. Tu-Sekine, M.S. Terrot, D. Trombino, T. Minh, E.S. Webster, R. Wilson, Eur. J. Med. Chem. **44**, 4169 (2009)
14. B.A. Al-Hiyari, A.K. Shakya, R.R. Naik, S. Bardaweel, Molbank **2021**, M1189 (2021)
15. C.U. Dueke-Eze, T.M. Fasina, A.E. Oluwalana, O.B. Familoni, J.M. Mphalele, C. Onubuogu, Sci. Afr. **9**, e00522 (2020)
16. Y. Li, F. Zaera, Catal. Sci. Technol. **5**, 3773 (2015)
17. A. Riisio, A. Lehtonen, M.M. Hanninen, R. Sillanpaa, Eur. J. Inorg. Chem. **2013**, 1499 (2013)
18. R. Bikas, V. Lippolis, N. Noshiranzadeh, H. Farzaneh-Bonab, A.J. Blake, M. Siczek, H. Hosseini-Monfared, T. Lis, Eur. J. Inorg. Chem. **2017**, 999 (2017)
19. M.M. Javadi, M. Moghadam, I. Mohammadpoor-Baltork, S. Tangestaninejad, V. Mirkhani, H. Kargar, M.N. Tahir, Polyhedron **72**, 19 (2014)
20. C.R. Craig, R.E. Stitzel, *Modern Pharmacology with Clinical Applications*, 6th edn. (Lippincott Williams & Wilkins, Baltimore, 2004)
21. S.A. Blum, R.G. Bergman, J.A. Ellman, J. Org. Chem. **68**, 150 (2003)
22. J. Fink, *High Performance Polymers*, 2nd edn. (William Andrew Inc., Norwich, 2008)
23. I. Fernandez, N. Khair, Chem. Rev. **103**, 3651 (2003)
24. M. Bagherzadeh, L. Tahsini, R. Latifi, A. Ellern, L.K. Woo, Inorg. Chim. Acta **361**, 2019 (2008)
25. N.Y. Jin, J. Coord. Chem. **65**, 4013 (2012)
26. L. Wang, Y.J. Han, Q.B. Li, L.W. Xue, Russ. J. Coord. Chem. **43**, 389 (2017)
27. A. Sigel, H. Sigel (eds.), *Handbook on Metalloproteins* (Marcel Dekker, New York, 2002)
28. J.M. Tunney, J. McMaster, C.D. Garner, in *Comprehensive Coordination Chemistry II*, ed. by J.A. McCleverty, T.J. Meyer (Elsevier Pergamon, Amsterdam, 2004)
29. C.G. Young, in *Encyclopedia of Inorganic Chemistry 2*, ed. by R.B. King (Wiley, Chichester, 2005)
30. C.J. Doonan, D.J. Nielsen, P.D. Smith, J.M. White, G.N. George, C.G. Young, J. Am. Chem. Soc. **128**, 305 (2006)
31. B.K. Burgess, in *Metal Ions in Biology Series, Molybdenum Enzymes*, ed. by T.G. Spiro (Wiley-Interscience, New York, 1985)
32. H. Kargar, M. Bazrafshan, M. Fallah-Mehrjardi, R. Behjatmanesh-Ardakani, H.A. Rudbari, K.S. Munawar, M. Ashfaq, M.N. Tahir, Polyhedron **202**, 115194 (2021)
33. H. Kargar, P. Foroootan, M. Fallah-Mehrjardi, R. Behjatmanesh-Ardakani, H.A. Rudbari, K.S. Munawar, M. Ashfaq, M.N. Tahir, Inorg. Chim. Acta **523**, 120414 (2021)
34. R. Kia, H. Kargar, J. Coord. Chem. **68**, 1441 (2015)
35. C. Radunsky, J. Kosters, M.C. Letzel, S. Yogendra, C. Schwickert, S. Manck, B. Sarkar, R. Pottgen, J.J. Weigand, J. Neugebauer, J. Muller, Eur. J. Inorg. Chem. **2015**, 4006 (2015)
36. V. Mirkhani, S. Tangestaninejad, M. Moghadam, I. Mohammadpoor-Baltork, H. Kargar, J. Mol. Catal. A: Chem. **242**, 251 (2005)
37. M. Hatefi, M. Moghadam, I. Sheikhshoei, V. Mirkhani, S. Tangestaninejad, I. Mohammadpoor-Baltork, H. Kargar, Appl. Catal. A: Gen. **370**, 66 (2009)
38. H. Kargar, Inorg. Chem. Commun. **14**, 863 (2011)
39. H. Kargar, Transition Met. Chem. **39**, 811 (2014)
40. G.J.J. Chen, J.W. McDonald, W.E. Newton, Inorg. Chem. **15**, 2612 (1976)
41. Stoe & Cie, X-Area, version 1.30: Program for the acquisition and analysis data (Stoe & Cie GmbH, Darmstadt, 2005)
42. R.H. Blessing, Acta Crystallogr. A **51**, 33 (1995)
43. A.L. Spek, Acta Crystallogr. **D65**, 148 (2009)
44. G.M. Sheldrick, Acta Crystallogr. A **64**, 112 (2008)
45. S.P. Gao, J. Coord. Chem. **64**, 2869 (2011)
46. Y.M. Cui, Y. Wang, Y.J. Cai, X.J. Long, W.J. Chen, Coord. Chem. **66**, 2325 (2013)
47. V. Vrdoljak, B. Prugovecki, D.M. Calogovic, J. Pisk, R. Dreos, P. Siega, Cryst. Growth Des. **11**, 1244 (2011)
48. M. Bagherzadeh, M. Amini, H. Parastar, M. Jalali-Heravi, A. Ellern, L.K. Woo, Inorg. Chem. Commun. **20**, 86 (2012)
49. A. Rana, R. Dinda, P. Sengupta, S. Ghosh, L.R. Falvello, Polyhedron **21**, 1023 (2002)
50. S. Gao, X.F. Zhang, L.H. Huo, H. Zhao, Acta Crystallogr. **E60**, m1731 (2004)
51. V. Vrdoljak, M. Cindric, D. Milic, D. Matkovic-Calogovic, P. Novak, B. Kamenar, Polyhedron **24**, 1717 (2005)
52. M. Karman, M. Wera, G. Romanowski, Polyhedron **187**, 114653 (2020)